

# Flavours of dark matter

Raymond R. Volkas

ARC Centre of Excellence for Dark Matter Particle Physics (CDM)

The University of Melbourne



1. Brief introduction

2. VISHv: axion DM,  $\nu$  masses, leptogenesis, inflation, flavoured Higgs

3. Cosmological coincidence, asymmetric DM, IR fixed points

4. Closing remarks

Sopov, RV: VISHv: a unified solution to five SM shortcomings with a protected electroweak scale. arXiv:2206.11598

Ritter, RV: Exploring the cosmological coincidence using infrared fixed points. PRD 107 (2023) 1, 015029

# 1. Brief introduction

The discovery of dark matter could be the discovery of a hidden sector!

I sincerely hope that colliders discover new physics one day soon.

But maybe one reason they haven't so far is that a lot of new physics is hidden ... I've been of this view for many years now, driven by the circumstantial evidence.

What do we know about DM?

It exists. It gravitates.

It doesn't interact much with ordinary matter.

So far, it appears to be collisionless.

It was at most warm when it facilitated structure formation.

$$\Omega_{\text{DM}} \simeq 5 \Omega_{\text{VM}}.$$

A (small) selection of what we don't know:

One particle or part of a full hidden sector?

Any connection with other mysteries?

Fermion or boson or PBH?

Elementary or composite or PBH?

Mass?

Any non-gravitational couplings?

⋮



## 2. VISHv: axion DM, $\nu$ masses, leptogenesis, inflation, flavoured Higgs

Based on the Dine-Fischler-Srednicki-Zhitniksii (DFSZ) axion model (1980, 1981): Peccei-Quinn symmetry.  
Invisible axion.  
Two Higgs doublets.  
PQ singlet scalar.  
No exotic fermions.

Successes of DFSZ model: (i) solves the strong CP problem  
(ii) provides axion DM candidate for PQ scale of  $10^{10} - 10^{11}$  GeV

Obvious extension: identify PQ and type-I seesaw scales and (iii) explain  $\nu$  masses

Langacker, Peccei, Yanagida (1986)  
Shin (1987)

Then also: (iv) explain baryogenesis via type-I seesaw leptogenesis

Langacker, Peccei, Yanagida (1986)  
Fukugita, Yanagida (1986)

Cosmological challenges: (a) Tension between Davidson-Ibarra and Vissani bounds

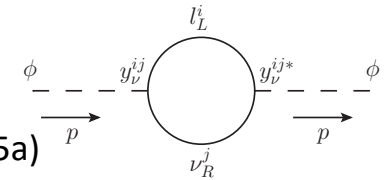
$$M_N > 5 \times 10^8 - 2 \times 10^9 \text{ GeV}$$

$$M_N < 3 \times 10^7 \text{ GeV}$$

For sufficient CPV with hierarchical N masses

Davidson, Ibarra (2002)  
Giudice+ (2004)

Vissani (1998)  
Clarke, Foot, RV (2015a)



Resolved in DFSZ using freedoms allowed by having two Higgs doublets: the vDFSZ model.

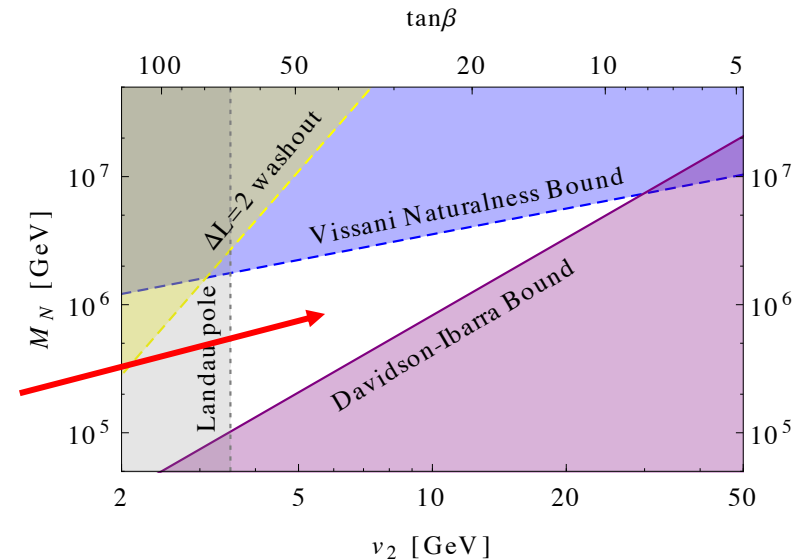
Clarke, Foot, RV (2015b)  
Clarke, RV (2016)

$H_1$  couples to up-type quarks.  $H_2$  to neutrinos and down-type quarks.

Induced VEV for  $H_2$  so that  $v_2 \ll v_1$ .

Vissani and DI bounds scale differently with  $v_2$ .

Allowed region



(b) Standard DFSZ has a cosmological domain wall problem.

Sikivie (1982)

Resolved through certain flavour-dependent quark Yukawa couplings to the Higgs doublets.

The “top specific” example has been analysed in the literature.

Bonus: rationale for why top is the most massive fermion.

Pheno signatures:  $t \rightarrow cH$ ,  $uH$ .

Peccei, Wu, Yanagida (1986)

Krauss, Wilczek (1986)

Chiang+ (2015, 2018)

Davidson, Vozmediano (1984a, 1984b)

Geng, Ng (1989, 1990)

Hayat (MSc thesis, UoM, 2022)

Diehl, Koutsangelas (2023)

Dolan, Hayat, Thamm, RV (in progress)

(c) Need inflation (or an alternative?) to resolve cosmological fine-tuning and seed structure formation.

VISHv is a vDFSZ top-specific variant that incorporates successful inflation.

Sopov, RV (2022)

Related to a KSVZ axion implementation (aka SMASH):

Salvio (2015, 2019)

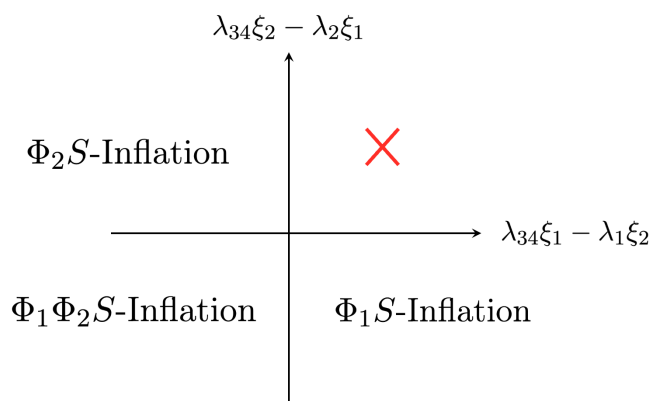
Ballesteros, Redondo, Ringwald, Tamarit (2017a, 2017b, 2019)

Like SMASH, we explore variants of “Higgs inflation”, through non-minimal couplings of scalar fields to gravity:

$$\frac{\mathcal{L}^{\mathcal{J}}}{\sqrt{-g^{\mathcal{J}}}} \supset \left( \frac{M_P^2}{2} + \xi_1 \Phi_1^\dagger \Phi_1 + \xi_2 \Phi_2^\dagger \Phi_2 + \xi_S S^\dagger S \right) R^{\mathcal{J}}$$

(J = Jordan frame)

$$\Phi_1^0 = \frac{\rho_1}{\sqrt{2}} e^{i\vartheta_1/v_1}, \quad \Phi_2^0 = \frac{\rho_2}{\sqrt{2}} e^{i\vartheta_2/v_2}, \quad S = \frac{\sigma}{\sqrt{2}} e^{i\vartheta_S/v_S}$$

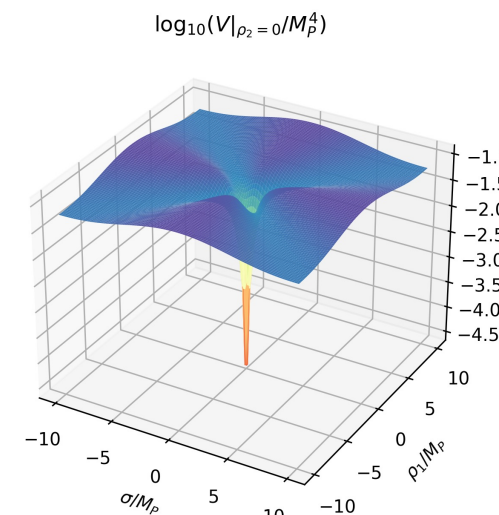


Example: different parameter regions produce different inflaton directions

Quartic potential becomes flat at large modulus field values in the Einstein frame: fits cosmological data very well.

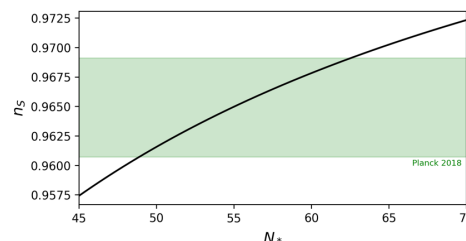
Inflatons  $\chi$  given by attractor valleys in the potential:

$$V^{\mathcal{E}}(\chi) \simeq \frac{M_P^4}{8} \frac{\lambda_{\text{eff}}}{\xi_{\text{eff}}^2} \left[ 1 - e^{-\frac{2}{\sqrt{6}} \frac{\chi}{M_P}} \right]^2$$

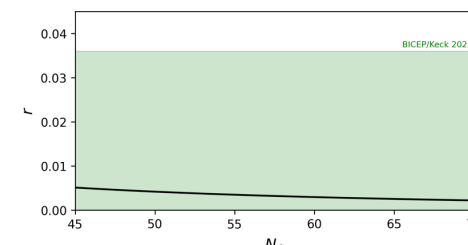


Fit to cosmo observables:

$$\frac{\lambda_{\text{eff}}}{\xi_{\text{eff}}^2} \sim 8.9 \times 10^{-10} \quad \text{scalar amplitude}$$



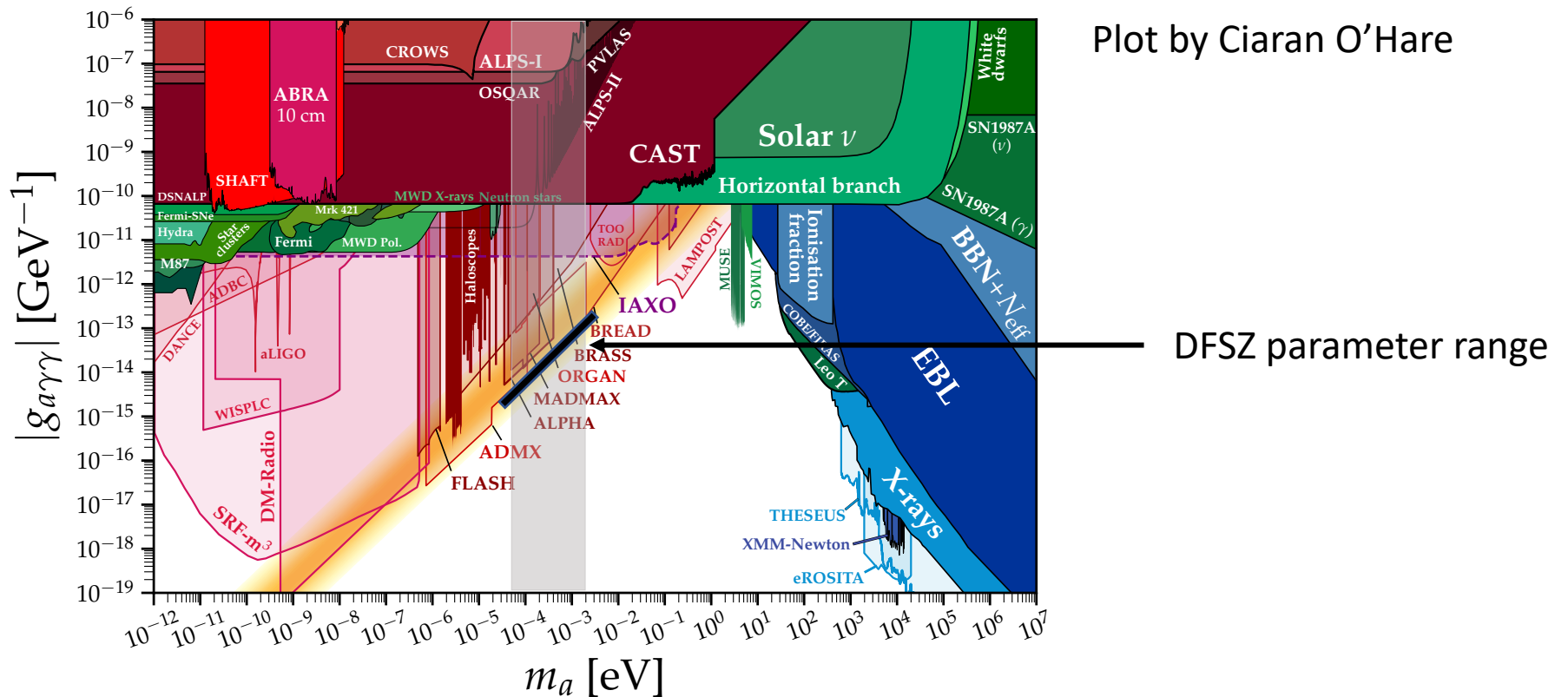
scalar spectral index



scalar-to-tensor ratio

**Signatures:** (a) axion DM, (b) additional EW Higgs states, (c)  $t \rightarrow cH, uH$ , (d) cosmo fits remaining good.

On-going work on pre- and re-heating.



$$m_A \sim (40 - 500) \mu\text{eV} \text{ for DM density}$$

$$m_A \in (40 \mu\text{eV}, \sim 2 \text{ meV})$$

full allowed range

### 3. Cosmological coincidence, asymmetric DM, IR fixed points

Ritter, RV (2023)

Asymmetric DM is motivated by the cosmological coincidence  $\Omega_{\text{DM}} \simeq 5\Omega_{\text{VM}}$

$$\rho_{\text{DM}} = m_{\text{DM}} n_{\text{DM}} \simeq 5\rho_{\text{VM}} = 5m_{\text{VM}} n_{\text{VM}}$$

But why is the DM mass scale related to the proton mass?  
Neglected topic.

chemically relate this to  $n_{\text{VM}}$  – staple of the ADM literature

proton mass: set by QCD scale

baryon asymmetry

Most obvious hypothesis: There is a dark QCD.  
Its confinement scale is related to normal QCD scale.  
DM is a (stable) “dark neutron”.

But how may the dark and normal confinement scales be related?

Answer #1: A  $Z_2$  symmetry between  $SU(3)_{\text{QCD}}$  and  $SU(3)_{\text{dQCD}}$ .  
Widely explored in the literature through mirror matter models.

Very incomplete list of citations going back to the 1950s:

Lee, Yang  
Kobzarev, Okun, Pomeranchuk  
Foot, Lew, RV  
Bereziani, Mohapatra  
Bereziani, Comelli, Villante  
Others by Bereziani et al  
Foot, RV  
Many papers by Foot ...  
Lonsdale, RV  
Ritter, RV

I wanted to explore a new idea.  
One has been provided by Bai and Schwaller (2014).

The Bai-Schwaller idea: No  $Z_2$  between QCD and dQCD.

Instead the two running couplings evolve to a common IR fixed point.

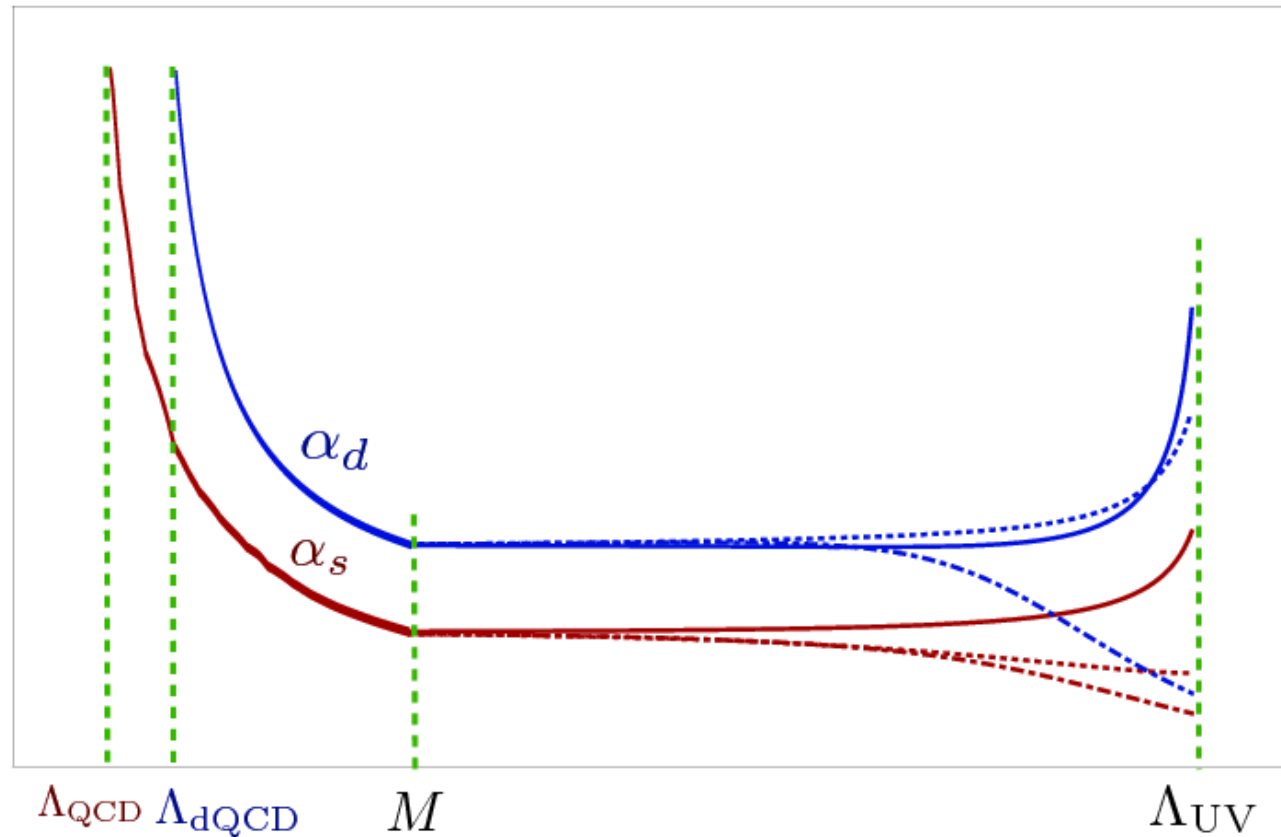


Figure from Bai and Schwaller paper.



My PhD student Alex Ritter and I decided to look at this interesting idea more closely.

DM is bound state of  
the light dark quarks

Field	$SU(3)_{\text{QCD}} \times SU(3)_{\text{dQCD}}$	Mass	Multiplicity
Fermion	$(\mathbf{3}, \mathbf{1})$	$M$	$n_{f_{c,h}}$
	$(\mathbf{1}, \mathbf{3})$	$< \Lambda_{\text{dQCD}}$	$n_{f_{d,l}}$
		$M$	$n_{f_{d,h}}$
	$(\mathbf{3}, \mathbf{3})$	$M$	$n_{f_j}$
Scalar	$(\mathbf{3}, \mathbf{1})$	$M$	$n_{s_c}$
	$(\mathbf{1}, \mathbf{3})$	$M$	$n_{s_d}$
	$(\mathbf{3}, \mathbf{3})$	$M$	$n_{s_j}$

TABLE I. The new particle content in a model. The given multiplicities are for Dirac fermions and complex scalars. A subscript containing  $l$  ( $h$ ) indicates a multiplicity for light (heavy) particles in cases where this is a relevant distinction to make.

$$\begin{aligned} \beta_c = & \frac{g_c^3}{16\pi^2} \left[ \frac{2}{3} (n_{f_c} + 3n_{f_j}) + \frac{1}{6} (n_{s_c} + 3n_{s_j}) - 11 \right] \\ & + \frac{g_c^5}{(16\pi^2)^2} \left[ \frac{38}{3} (n_{f_c} + 3n_{f_j}) + \frac{11}{3} (n_{s_c} + 3n_{s_j}) - 102 \right] \\ & + \frac{g_c^3 g_d^2}{(16\pi^2)^2} [8n_{f_j} + 8n_{s_j}], \quad \beta_d \text{ obtained by } c \leftrightarrow d \end{aligned}$$

condition for fixed point:

$$\beta_c(g_c^*, g_d^*) = \beta_d(g_c^*, g_d^*) = 0.$$

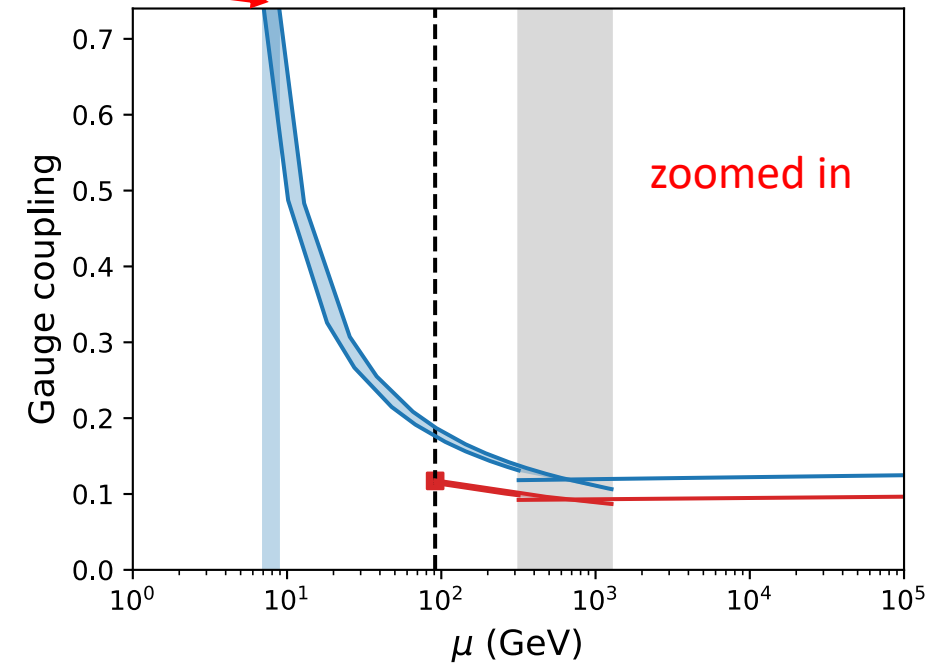
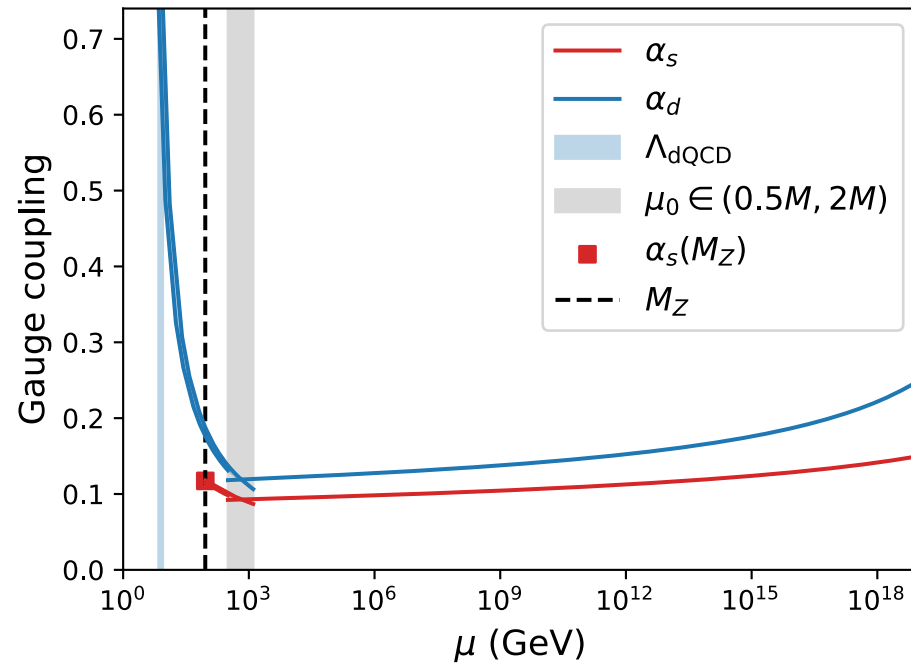
We initially stick to multiplicities  $\leq 3$

We extended the Bai-Schwaller analysis in a number of ways:

(a) Used 1-loop matching of the IR and UV theories. Have matching scale  $\mu_0$  as well as NP scale  $M$ . Keep  $\mu_0$  between  $0.5M$  and  $2M$  to suppress large logs.

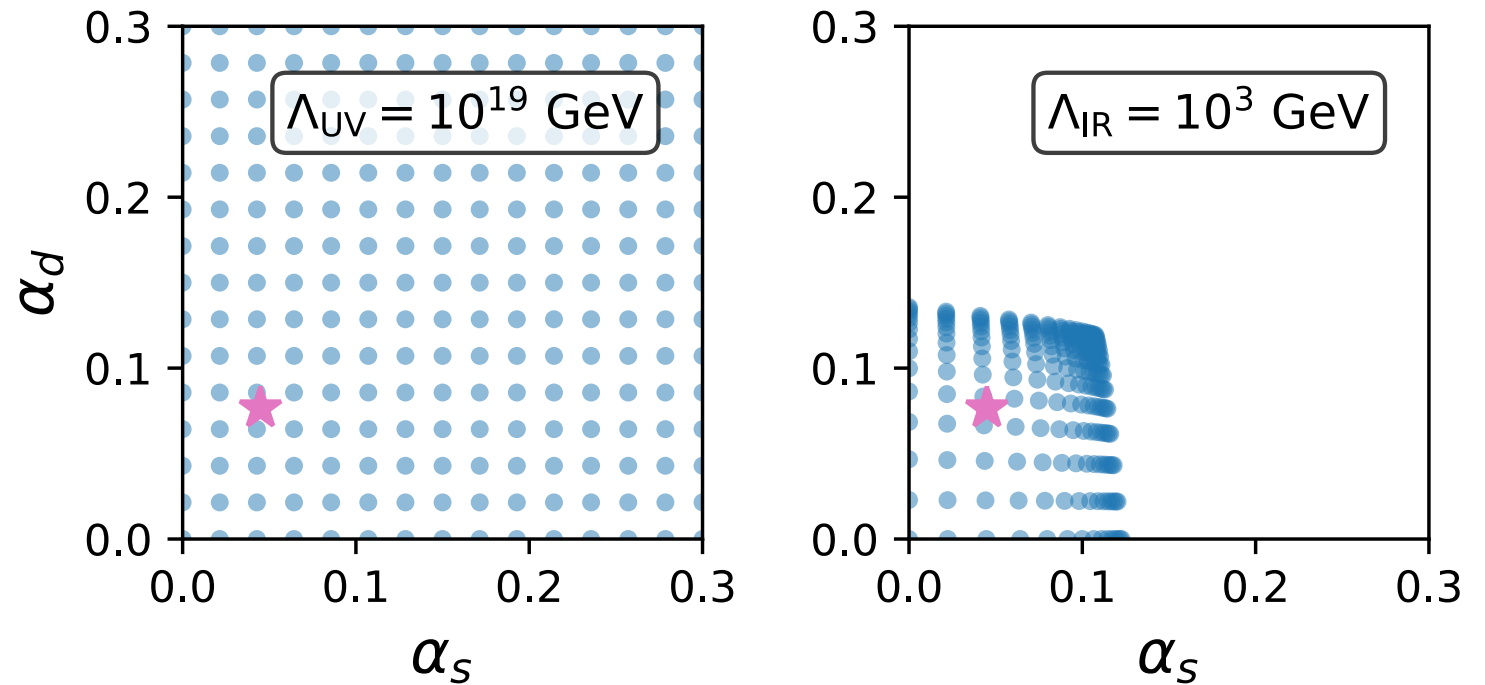
Newstead, TerBeek (2014)

Get range of  $\Lambda_{\text{dQCD}}$  as  $\mu_0$  is varied

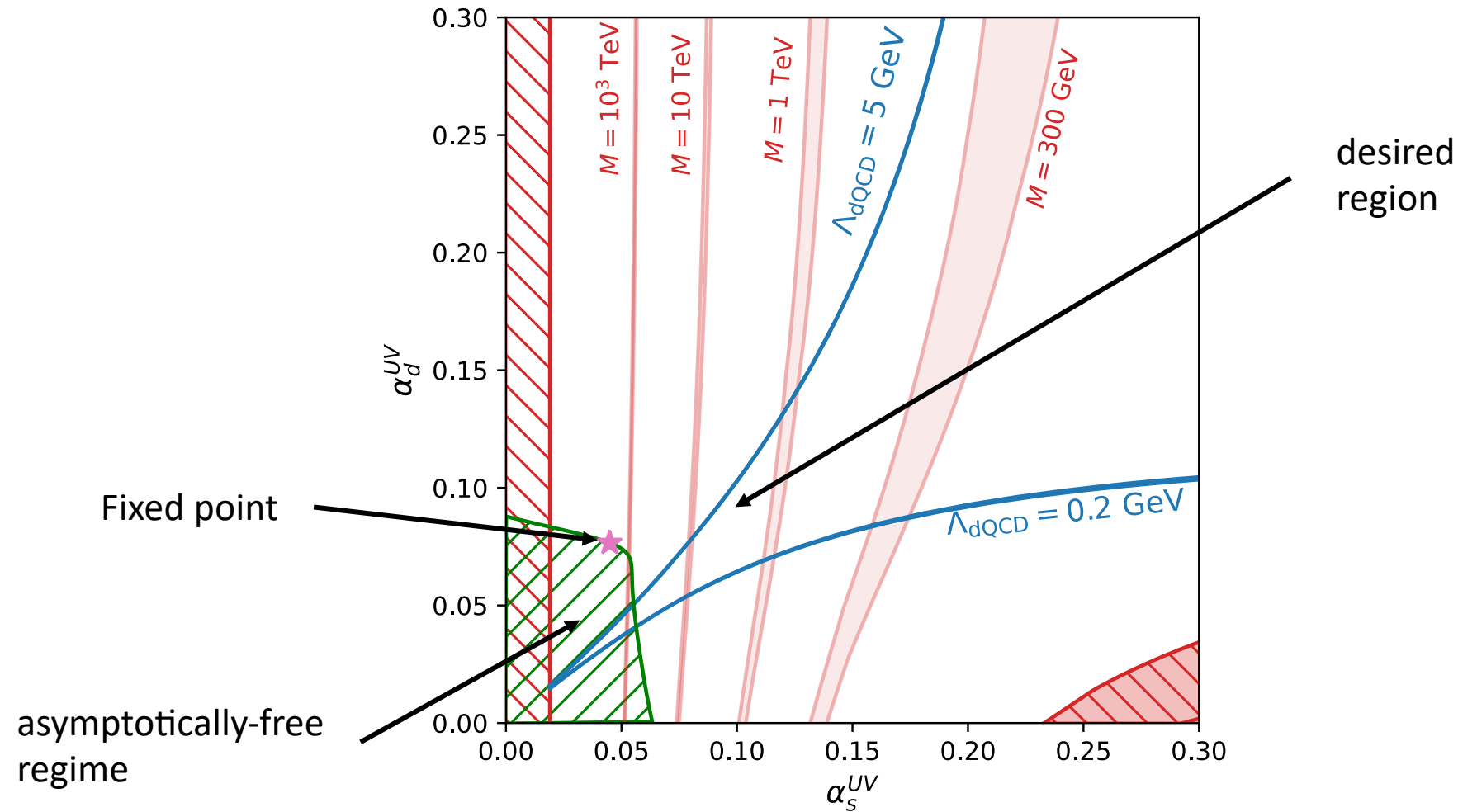


(b) Computed residual dependence on initial conditions. The running couplings approach but do not attain their FP values.

An example. Pink star is the fixed point.

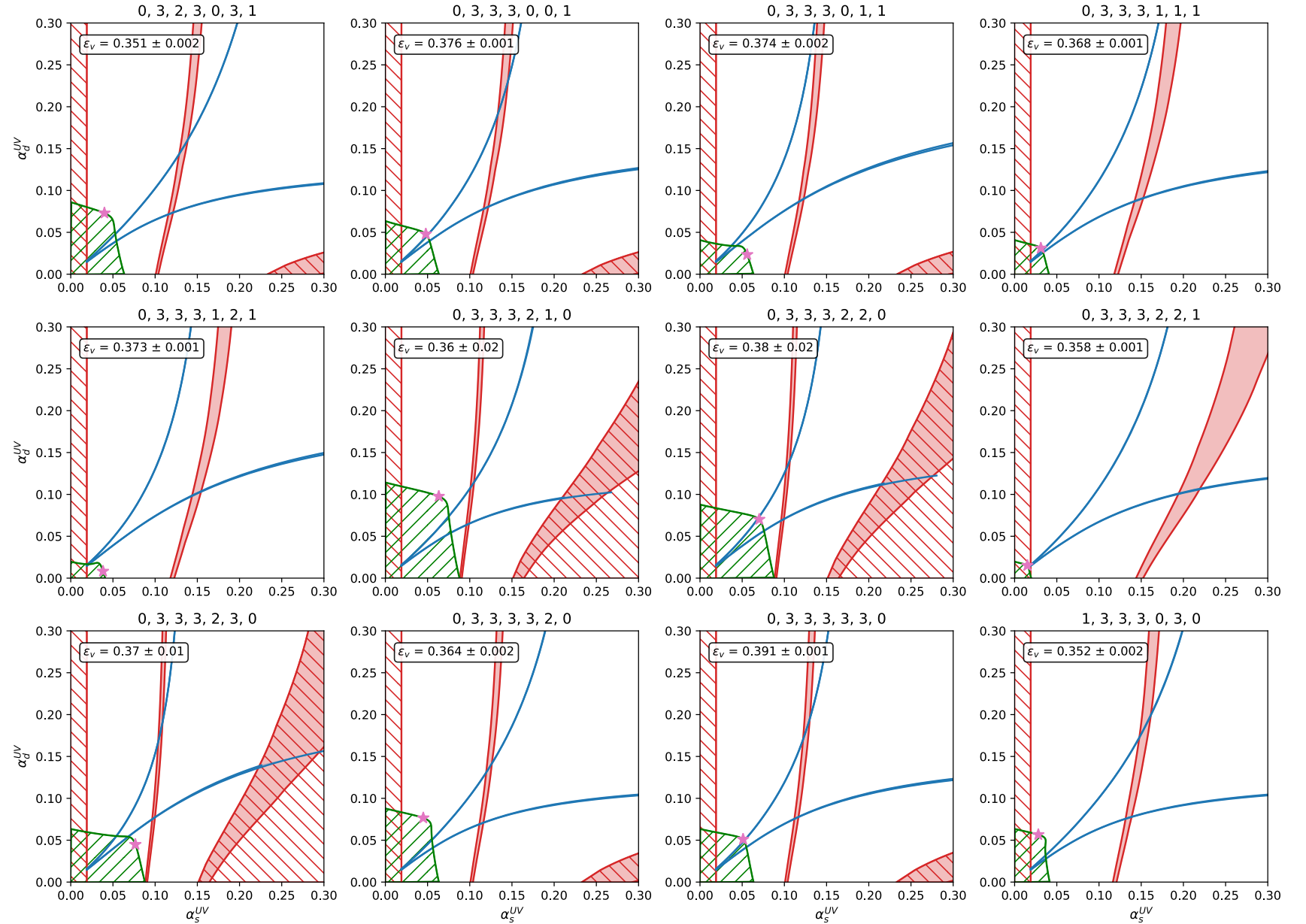
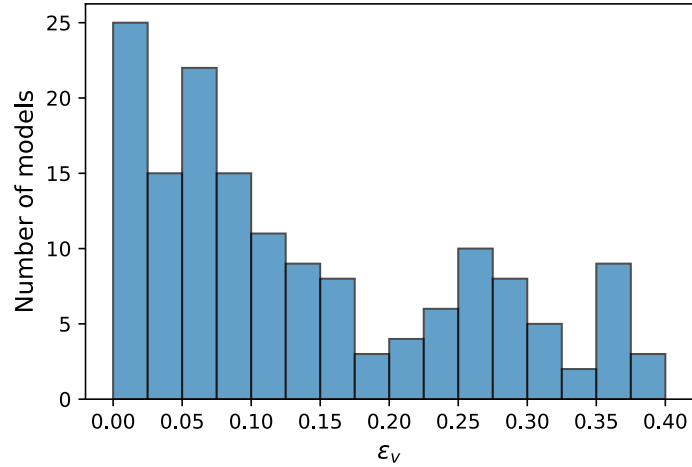


(c) Computed a “validity fraction”: the fraction of parameter space giving  $0.2\Lambda_{\text{QCD}} < \Lambda_{\text{dQCD}} < 5\Lambda_{\text{QCD}}$



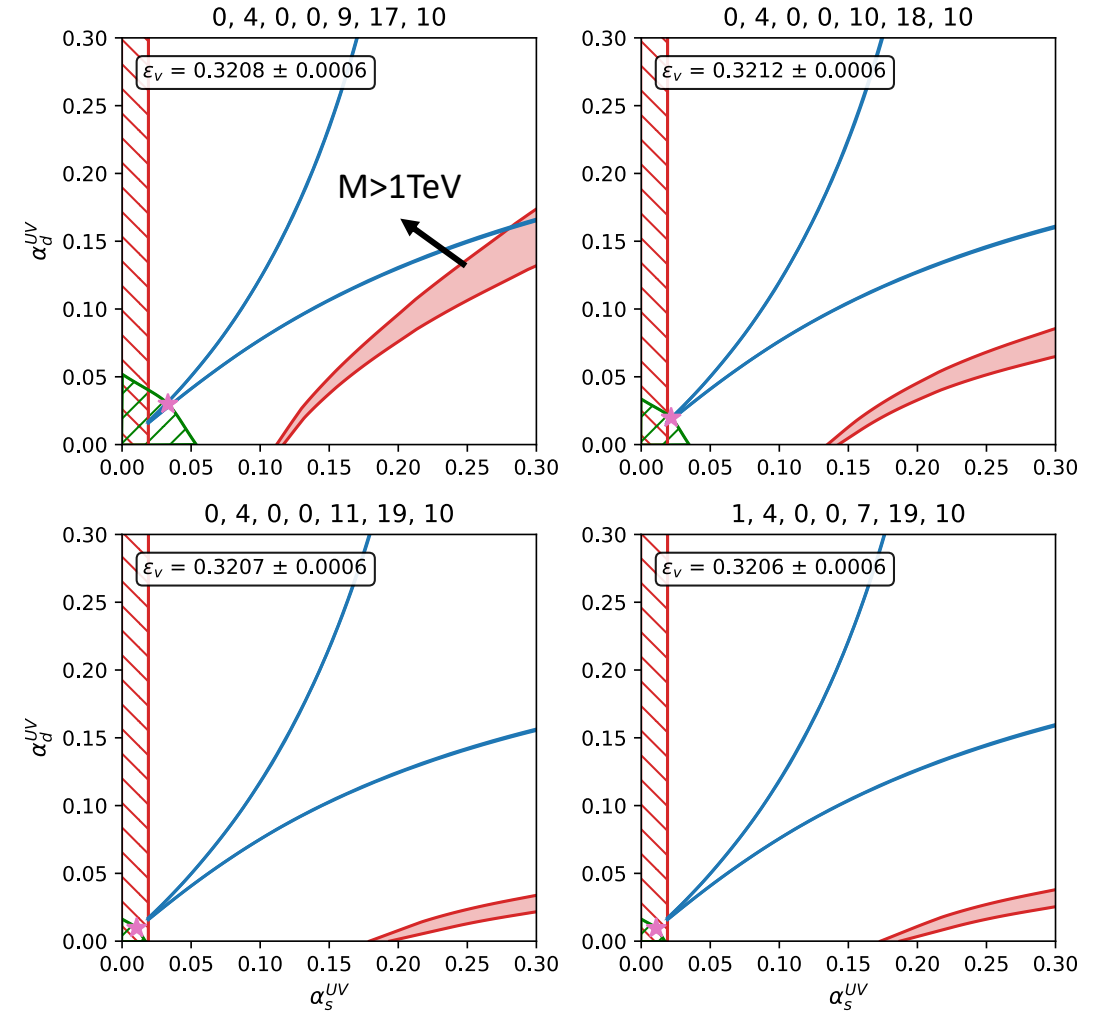
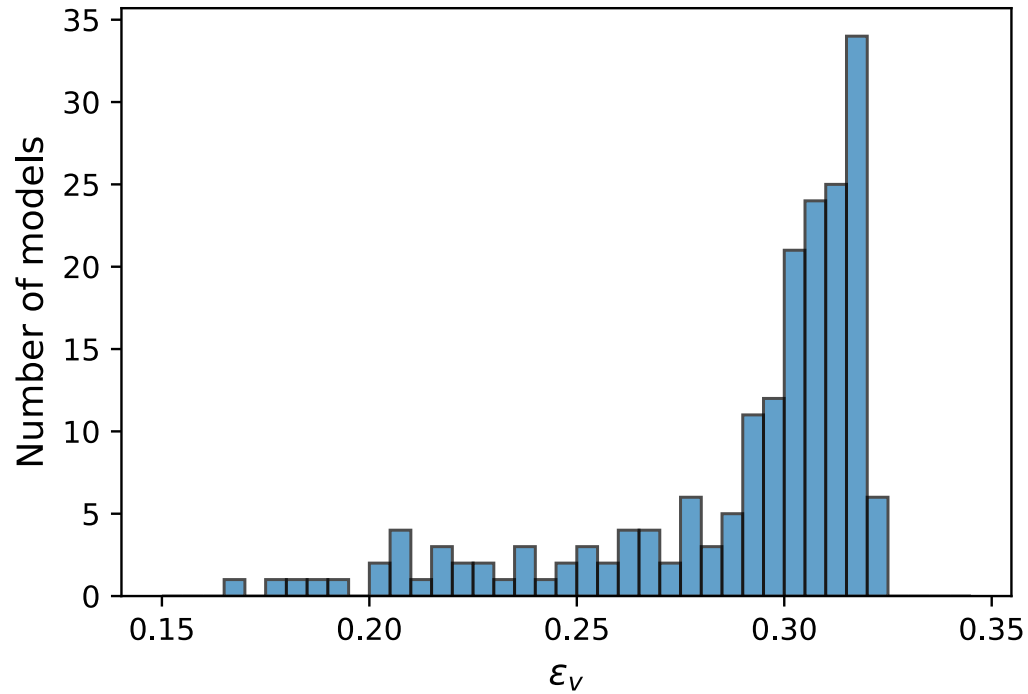
Models with the highest validity fractions  $\epsilon_v$ .

However, a lot of the parameter space requires  $NP < 1$  TeV, which is ruled out.



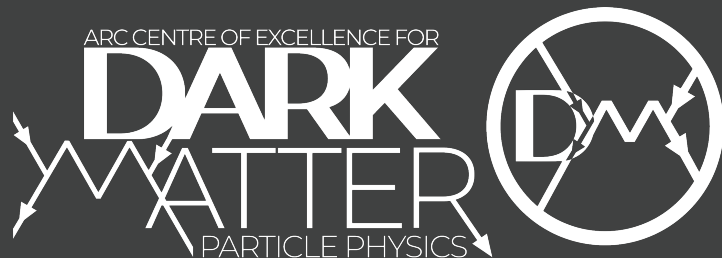
(d) To get larger values of  $M$ : need stronger running from UV scale to  $M$  – increase multiplicity of some multiplets.

Examples:



## 4. Closing remarks

- VISHv (and SMASH) are interesting, economical models for solving 5 important problems.
  - VISHv uses interesting PQ/flavour interplay to avoid domain wall problem (1980s!).
  - Higgs/S inflation works well. (P)reheating analysis is on-going work.
- 
- The Bai-Schwaller idea is an interesting framework for asymmetric DM model-building.
  - We have only taken baby steps in exploring the possible models ...



**Australian Government**  
**Australian Research Council**

## National Partners



**Australian National University**



THE UNIVERSITY OF  
**SYDNEY**



**Australian Government**  
**Department of Defence**



Australian Government



## International Partners



UvA



**Stockholm University**



The University  
Of  
Sheffield.





# BACK-UP SLIDES

## The vDFSZ model:

Clarke, RV (2016)

Take the 2HDM, add three RH neutrinos and a complex scalar singlet  $S$ , impose Peccei-Quinn symmetry.  
Axion is the phase of  $S$ .

$$-\mathcal{L}_Y = y_u \bar{q}_L \tilde{\Phi}_1 u_R + y_d \bar{q}_L \Phi_2 d_R + y_e \bar{\ell}_L \Phi_J e_R + y_\nu \bar{\ell}_L \tilde{\Phi}_2 \nu_R + \frac{1}{2} y_N \overline{(\nu_R)^c} S \nu_R + h.c.$$

J=2 (1) is Type-II (Flipped) v2HDM

generates  $M_N < 3 \times 10^7 \text{ GeV}$

$$V = M_{11}^2 \Phi_1^\dagger \Phi_1 + M_{22}^2 \Phi_2^\dagger \Phi_2 + M_{SS}^2 S^* S + \frac{\lambda_1}{2} (\Phi_1^\dagger \Phi_1)^2 + \frac{\lambda_2}{2} (\Phi_2^\dagger \Phi_2)^2 + \frac{\lambda_S}{2} (S^* S)^2 + \lambda_3 (\Phi_1^\dagger \Phi_1) (\Phi_2^\dagger \Phi_2) + \lambda_4 (\Phi_1^\dagger \Phi_2) (\Phi_2^\dagger \Phi_1) + \lambda_{1S} (\Phi_1^\dagger \Phi_1) (S^* S) + \lambda_{2S} (\Phi_2^\dagger \Phi_2) (S^* S) + \epsilon \Phi_1^\dagger \Phi_2 S^2 + h.c.$$

EW scale  $\sim -(88 \text{ GeV})^2$        $+(10^3 \text{ GeV})^2$       PQ scale  $\sim -(10^{11} \text{ GeV})^2$

tiny inter-sector couplings      induces linear term for  $\Phi_2$  and thus small  $v_2$

VISHv using the top-specific PQ charge assignment:

$q_L$	$u_R^a$	$u_R^3$	$d_R$	$l_L$	$e_R$	$\nu_R$	$\Phi_1$	$\Phi_2$	$S$
0	$-\sin^2 \beta$	$\cos^2 \beta$	$\sin^2 \beta$	$\frac{1}{2} - \cos^2 \beta$	$\frac{3}{2} - 2 \cos^2 \beta$	$-\frac{1}{2}$	$\cos^2 \beta$	$-\sin^2 \beta$	1

↑  
RH top has distinct PQ charge

Only  $\Phi_1$  couples to RH top

$$\begin{aligned}
 -\mathcal{L}_Y = & \overline{q}_L^j y_{u1}^{j3} \tilde{\Phi}_1 u_R^3 + \overline{q}_L^j y_{u2}^{ja} \tilde{\Phi}_2 u_R^a + \overline{q}_L^j y_d^{jk} \Phi_2 d_R^k + \overline{l}_L^j y_e^{jk} \Phi_2 e_R^k \\
 & + \overline{l}_L^j y_\nu^{jk} \tilde{\Phi}_2 \nu_R^k + \frac{1}{2} (\nu_R)^c y_N^{jk} S \nu_R^k + \text{h.c.}
 \end{aligned}$$

Collider signatures and constraints:  $t \rightarrow hc$  and  $t \rightarrow hu$   
 $cg \rightarrow tH$  or  $tA$  and  $cg \rightarrow bH^+$

Chiang+ (2015, 2018)  
Hou, Modak (2021)  
Ghosh, Hou, Modak (2020)  
Kohda, Modak, Hou (2018)

Like SMASH, we explore variants of “Higgs inflation”, through non-minimal couplings of scalar fields to gravity:

$$\frac{\mathcal{L}^{\mathcal{J}}}{\sqrt{-g^{\mathcal{J}}}} \supset \left( \frac{M_P^2}{2} + \xi_1 \Phi_1^\dagger \Phi_1 + \xi_2 \Phi_2^\dagger \Phi_2 + \xi_S S^\dagger S \right) R^{\mathcal{J}} \quad (\text{J = Jordan frame})$$

$$\text{Let} \quad \Phi_1^0 = \frac{\rho_1}{\sqrt{2}} e^{i\vartheta_1/v_1}, \quad \Phi_2^0 = \frac{\rho_2}{\sqrt{2}} e^{i\vartheta_2/v_2}, \quad S = \frac{\sigma}{\sqrt{2}} e^{i\vartheta_S/v_S}$$

$$\text{Go to Einstein (E) frame:} \quad g_{\mu\nu}^{\mathcal{J}} \rightarrow g_{\mu\nu}^{\mathcal{E}} = \Omega^2(\rho_1, \rho_2, \sigma) g_{\mu\nu}^{\mathcal{J}} \quad \text{where} \quad \Omega^2 \equiv 1 + \frac{\xi_1 \rho_1^2 + \xi_2 \rho_2^2 + \xi_S \sigma^2}{M_P^2}.$$

$$\text{Then:} \quad \frac{\mathcal{L}^{\mathcal{E}}}{\sqrt{-g^{\mathcal{E}}}} \supset \frac{M_P^2}{2} R^{\mathcal{E}} - \frac{1}{2} \mathcal{G}_{IJ}^{\mathcal{E}} \partial_\mu \varphi^I \partial^\mu \varphi^J - V^{\mathcal{E}}(\varphi^I)$$

$$V^{\mathcal{E}}(\varphi^I) = \Omega^{-4}(\varphi^I) V^{\mathcal{J}}(\varphi_I) \simeq \frac{M_P^4}{8} \frac{\lambda_i \rho_i^4 + 2\lambda_{34} \rho_1^2 \rho_2^2 + 2\lambda_{iS} \rho_i^2 \sigma^2 + \lambda_S \sigma^4}{(M_P^2 + \xi_i \rho_i^2 + \xi_S \sigma^2)^2} \quad (\lambda_{34} \equiv \lambda_3 + \lambda_4)$$

Potential is flat at large moduli: good for inflation

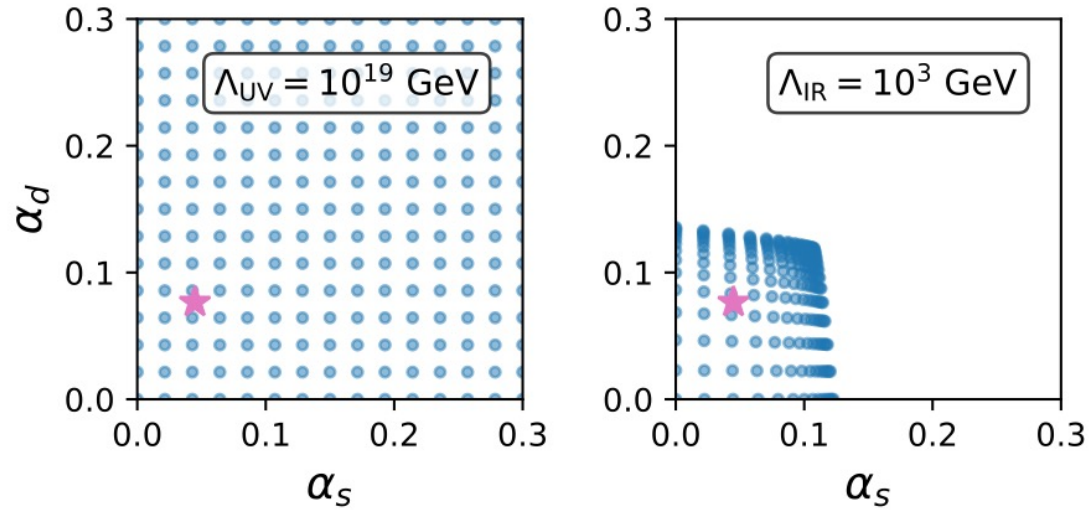


FIG. 1. **Left:** A grid of values for the strong coupling constant  $\alpha_s$  and the dark coupling constant  $\alpha_d$  at an energy scale  $\Lambda_{UV} = 10^{19} \text{ GeV}$ . The pink star shows the infrared fixed point  $(\alpha_s^*, \alpha_d^*) = (0.045, 0.077)$  for the model with field multiplicities  $(n_{f_{c,h}}, n_{f_{d,l}}, n_{f_{d,h}}, n_{f_j}, n_{s_c}, n_{s_d}, n_{s_j}) = (3, 3, 3, 3, 3, 2, 0)$ . **Right:** The grid of values from the left panel has been evolved down from  $10^{19} \text{ GeV}$  to an energy scale  $\Lambda_{IR} = 10^3 \text{ GeV}$  under the RGEs of the given model. The pink star again indicates the IRFP of the model.

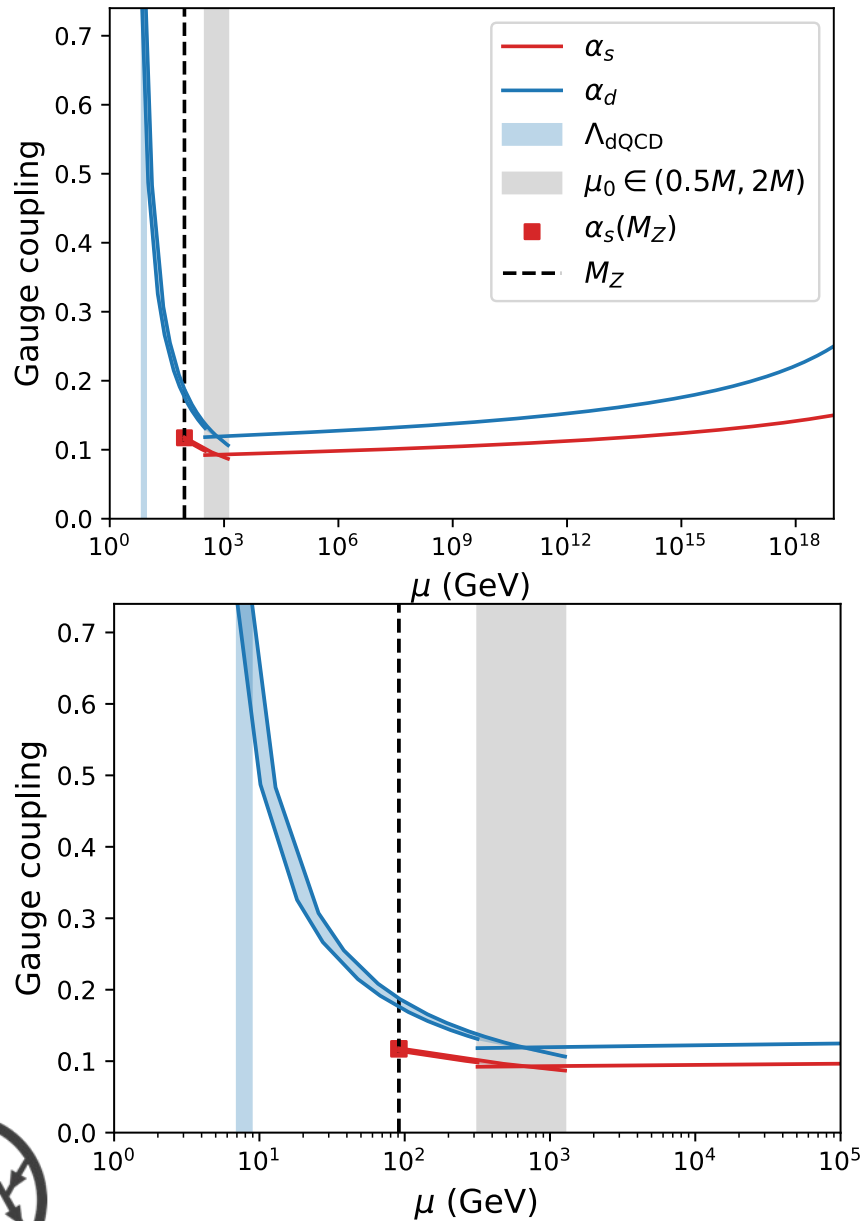


FIG. 2. **Top:** The evolution of the QCD and dQCD coupling constants for the model  $(n_{f_{c,h}}, n_{f_{d,l}}, n_{f_{d,h}}, n_{f_j}, n_{s_c}, n_{s_d}, n_{s_j}) = (3, 3, 3, 3, 3, 2, 0)$  with mass scale  $M = 635$  GeV and initial UV couplings  $(\alpha_s^{\text{UV}}, \alpha_d^{\text{UV}}) = (0.15, 0.25)$ . The mass scale is chosen so that  $\alpha_s$  obtains its measured value at  $M_Z$ , as indicated by the red square. The decoupling scale  $\mu_0$  is shown by the grey shaded band, where we allow it to vary between  $0.5M$  and  $2M$  to account for the uncertainty introduced by threshold corrections. Below the decoupling scale,  $\alpha_s$  and  $\alpha_d$  are depicted as bands, due to the variance in the decoupling scale. The vertical blue band indicates the range of values for the dark confinement scale  $\Lambda_{\text{dQCD}}$ , calculated as the energy scale where  $\alpha_d = \pi/4$ . **Bottom:** The same evolution, zoomed in to the energy range between 1 GeV and  $10^5$  GeV to show the variance in the coupling constants below the decoupling scale more clearly.

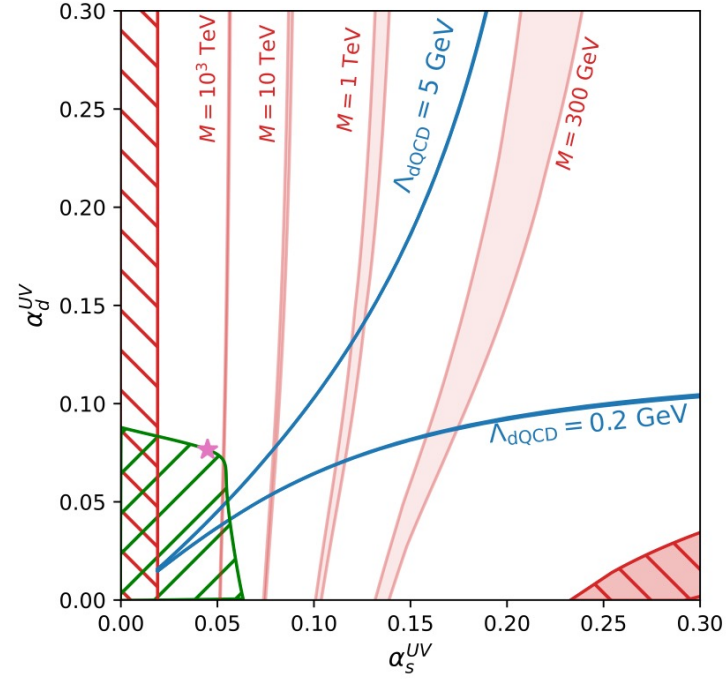


FIG. 3. For the model  $(n_{f_{c,h}}, n_{f_{d,l}}, n_{f_{d,h}}, n_{f_j}, n_{s_c}, n_{s_d}, n_{s_j}) = (3, 3, 3, 3, 3, 2, 0)$  we show contours for the dark confinement scale  $\Lambda_{\text{dQCD}}$  (blue) and for the new physics scale  $M$  (red) on axes of the initial UV couplings  $\alpha_s^{\text{UV}}$  and  $\alpha_d^{\text{UV}}$ . The width of these contours is due to the variance in the decoupling scale  $\mu_0$  between  $0.5M$  and  $2M$  to account for the uncertainty introduced by threshold corrections. In the red hatched regions there are no allowed values of  $M$  for which  $\alpha_s$  has the correct running at low energy. The pink star shows the infrared fixed point of this model. The green hatched region is the ‘asymptotically free’ region, where  $SU(3)_{\text{QCD}}$  and  $SU(3)_{\text{dQCD}}$  both exhibit asymptotic freedom.

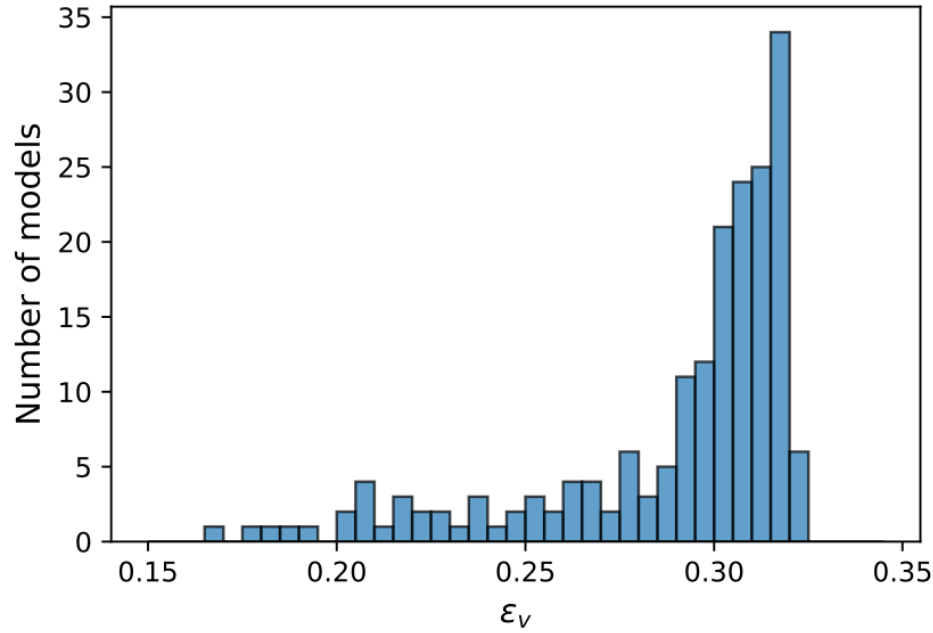


FIG. 9. A histogram of the validity fractions for the set of 188 models that have 10 or more joint scalars, and one-loop coefficients for the  $\beta$ -functions between  $-0.1$  and  $0$ . Each of these models has a mass scale  $M > 1$  TeV for at least 80% of the UV coupling parameter space.

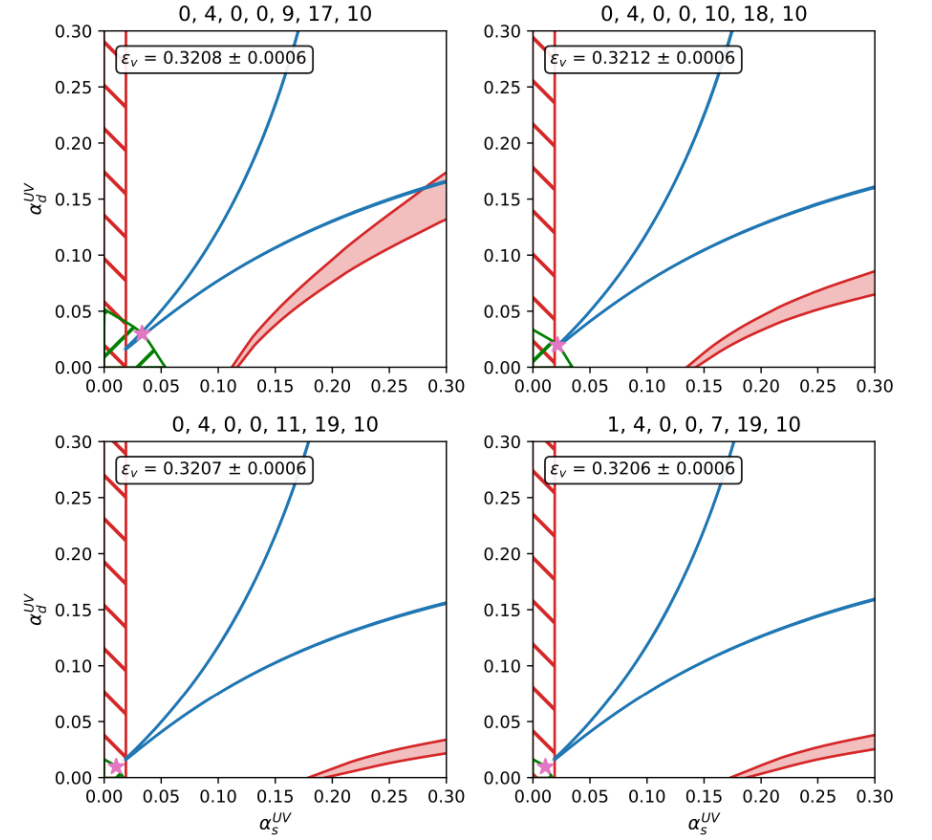


FIG. 10. The results for four models with  $\epsilon_v > 0.32$ . These are some of the models with the largest viability fraction in the set of 188 models shown in Fig. 9. The features of each subplot are the same as those in Fig. 6. Note that for each model, at least 80% of the parameter space has  $M > 1$  TeV, where  $M = 1$  TeV is shown by the red contour.